Leak detection in branched pipe systems coupling wavelet analysis and a Lagrangian model

Marco Ferrante, Bruno Brunone and Silvia Meniconi

ABSTRACT

Transient analysis of pressurized pipe systems yields useful information regarding the actual state in an effective and rapid manner and then it can be used for the diagnosis of the system. Besides the framework of the inverse problem solution, transient based leak detection can also focus on the modalities with which pressure waves generated by a known manoeuvre travel through a system. This latter approach has been successfully applied by several authors to simple systems, usually comprising a single pipe with a constant head reservoir and a valve at the end section. The present work extends this approach to more complex systems, that is, those with at least one junction. To accomplish this, the pressure signal is analysed using wavelet analysis, a technique which has produced encouraging results. Moreover, the analysis of the pressure signals is generalized by means of a Lagrangian model, which directly simulates the pressure waves' generations and movements in the system. Coupling wavelet analysis with the Lagrangian model allows us to associate singularities pointed out in pressure signals to singularities in the system. In order to better ascertain the applicability of the method, tests were carried out on both a laboratory installation and a real system.

Key words | leak detection, pressurized pipes, water hammer, wavelets

Marco Ferrante (corresponding author)
Bruno Brunone
Silvia Meniconi
Dipartimento di Ingegneria Civile ed Ambientale,
University of Perugia,
Via G. Duranti, 93-06125 Perugia,
Italy
Tel.: +39 075 585 3618
Fax: +39 075 585 3892
E-mail: *ferrante@unipg.it*

INTRODUCTION

Diagnosis of water distribution systems is a costly endeavour, in terms of both money and time. Despite this, utilities are evaluating the economics of system diagnosis more frequently than in the past, balancing the costs inherent in network investigation with the financial burden of operating their systems. As part of this general interest in assuring efficient system operation, attention to leak detection techniques which permit network investigation at diminished financial cost and time investment has grown. In striving to meet this objective, it has been shown that unsteady tests can yield information regarding current system state in a more effective and rapid manner than investigations based on steady state conditions (Liggett & Chen 1994). The first research activity focused on transient based leak detection was largely inspired by the work of Liggett & Chen (1994), in which the analysis of transient waves was undertaken in the context of formulating and solving an inverse problem, using numerical models incorporating the method of characteristics (MOC) solution scheme (a close examination of work in this vein was reported by Kapelan *et al.* 2003). Other work in transient based leak detection is distinguished by direct scrutiny of the modalities with which pressure waves generated by a known manoeuvre travel through a system. This later approach has been successfully applied by several authors to simple systems, usually comprising a single pipe with a constant head reservoir and a valve at opposite ends (Brunone 1989, 1999; Nicholas 1990; Jonsson & Larson 1992; Covas *et al.* 2000; Brunone & Ferrante 2001; Gudmundsson *et al.* 2002; Stephens *et al.* 2004).

In the real word many leak detection techniques exist because each one requires specific conditions and system

doi: 10.2166/aqua.2009.022

characteristics to trade off precision in sizing and locating, and costs. While the transient test based techniques can be performed at a very low cost per unit length of pipe, one of their limits is given by the system complexity, especially when the propagation of the pressure waves is analysed.

The present work extends the latter approach to branched systems (i.e. those with at least one junction), considering tests both in laboratory and in real pipe systems. To accomplish this, the pressure signal–that is, the pressure time-history in the measurement section–is analysed coupling a Lagrangian model and wavelet analysis, a technique which has produced encouraging results (Stoianov *et al.* 2001; Ferrante & Brunone 2003*b*; Brunone & Ferrante 2004; Ferrante *et al.* 2007).

THE LAGRANGIAN MODEL

The Lagrangian model is based on the D'Alembert's solution of the differential equations governing unsteady flow in pressurized pipes when the friction term is neglected. The omission of such a term is not limiting here since only the first phase of transient tests is considered and attention is focused on locating singularities.

With this assumption, the solution of the problem can be expressed as:

$$p - p^0 = F(t + s/a) + f(t - s/a) \tag{1}$$

$$V - V^0 = -\frac{1}{\rho a}[F(t + s/a) - f(t - s/a)] \tag{2}$$

where p and V are the pressure and mean velocity in a given instant t during the transient; the superscript 0 denotes the initial conditions, ρ is the density of fluid, a is the pressure wave speed. The functions $F(\ )$ and $f(\ )$ have dimensions of pressure and are arbitrary. They represent pressure waves that travel with velocity a along the directions $-s$ and $+s$, with s conforming to the direction of motion prior to the transient. Once determination of $F(\ )$ and $f(\ )$ is resolved, from Equations (1) and (2) it is possible to simulate the pressure at any section in the system; this, in fact, can be expressed as the cumulative sum of all the $F(\ )$ and $f(\ )$ that have passed that section up until that instant. The pressure at any section will remain constant in time until the passage of a wave, which causes a positive or negative change depending on the manoeuvre that gives rise to the transient or on the singularity that produces or reflects the wave. Thus, the proposed model, rather than determine the values of the pressure in prefixed sections and instants of time, memorizes the amplitude of each wave and the moment in which it passes the singularities. Consequently, having memorized the information regarding the movement of each wave, it is possible to simulate the behaviour in time of the pressure at any section in the system without constraint on position and in an essentially continuous manner.

It is worth nothing that the considered Lagrangian model resembles in many aspects that defined by the integration of the water hammer equations by the MOC. When the friction terms are neglected, the characteristic equations can be written as:

$$\begin{aligned} C^+ &\begin{cases} p - p^0 = -\rho a(V - V^0) \\ \frac{\mathrm{d}s}{\mathrm{d}t} = a \end{cases} \\ C^- &\begin{cases} p - p^0 = \rho a(V - V^0) \\ \frac{\mathrm{d}s}{\mathrm{d}t} = -a \end{cases} \end{aligned} \tag{3}$$

These equations coincide with those defined by Equations (1) and (2) when only waves propagating in the positive or in the negative direction are considered. They both represent an integration of the same partial differential equations. But while the MOC traces the waves along the system with a fixed Δt, while they propagated exactly for a Δs, the proposed method does not need a fixed time step and does not follow a definite, regular, time-space grid.

In the procedure, the first step is to define the topology of the system according to a graph: that is, an ensemble of links (i.e. branches of pipe in which characteristics do not vary) and nodes (i.e. sections where two or more links are connected and external flow exchanges may occur). For given topology and manoeuvre, the procedure requires us to send the pressure waves through the system, recording their paths and their arrival time at the nodes; then it is possible to reconstruct the signal at all sections of the system. Once the pressure change at a node is determined, the disturbance is transferred to other nodes by means of a transfer function that characterizes the link. In this case, the function is rather simple in that the wave (unchanged in its

amplitude) is transferred at the other extremity of the link after a time lag aL, with L being the length of the link. When the wave arrives at a node, it can be transmitted or reflected according to modalities that depend on its characteristics and that find a numerical expression in the coefficients of reflection and transmission. These coefficients are defined as the amplitude ratio between the reflected or transmitted wave, respectively, and the incident wave.

Consider, for example, a leak discharging in air at a node connecting links 1 and 2 for which Equations (1) and (2) become:+

$$\begin{cases} p_1^{t_L} - p_1^0 = F_1(\ ) + f_1(\ ) \\ p_2^{t_L} - p_2^0 = F_2(\ ) + f_2(\ ) \end{cases} \tag{4}$$

$$\begin{cases} Q_1^{t_L} - Q_1^0 = -\frac{A_1}{\rho a_1}(F_1(\ ) - f_1(\ )) \\ Q_2^{t_L} - Q_2^0 = -\frac{A_2}{\rho a_2}(F_2(\ ) - f_2(\ )) \end{cases} \tag{5}$$

where A_i and Q_i are, respectively, the cross-section area and the discharge at the i-th link, for $i = 1,2$. Assuming that an instantaneous total closure manoeuvre occurs on link 1, the overpressure $F_1(\ ) = \Delta p^* = \rho a V^0$ is transmitted upstream and reaches the leak at time t_L. The reflected wave in link 1 is $f_1()$ and the transmitted wave in link 2 is $F_2(\ )$, with $f_2(\ ) = 0$, since at such instant no reflected wave from link 2 can have reached the leak.

Should the most typical case of a leak situated in a pipe segment of constant diameter and uniform material be considered, combining Equations (4) and (5) with the continuity equation and assuming a common pressure at the leak, the following expression for the reflection coefficient is obtained:

$$C_{\mathrm{R}} = -\frac{I_r}{2 + I_r} \tag{6}$$

that for the transmission coefficient becomes:

$$C_{\mathrm{T}} = \frac{2}{2 + I_r} \tag{7}$$

in which $I_r = (Q_L^-/2Q_1^0)(\Delta p^*/p_L^-)$ (Ferrante & Brunone 2003*a*), where Q_L^- and p_L^- are the discharge through the leak and the pressure inside the pipe at the leak, respectively, before the pressure wave arrival. When the pressure wave generated by the manoeuvre is considered, $Q_L^- = Q_L^0$ and $p_L^- = p_L^0$.

The standard orifice equation has been used to model the leak hydraulic behaviour:

$$Q_L = k p_L^{\alpha} \tag{8}$$

where the leakage coefficient $k = C_L A_L (2/\rho)^{\alpha}$, C_L and A_L are the discharge coefficient and the area of the leak, p_L is the pressure inside the pipe at the leak, with $\alpha = 1/2$. It is worth noting that an exponent α equal to 1/2 seems to apply only in some circumstances: that is, when round holes or circumferential cracks are considered. Other leak geometries (e.g. longitudinal cracks and corrosion clusters), combined with specific pipe material properties or leak flow regimes, can produce higher values for α (Greyvenstein & van Zyl 2007; van Zyl & Clayton 2007). For a generic value of α, Equation (6) becomes:

$$C_R = -\frac{I_r}{\alpha^{-1} + I_r} \tag{9}$$

The reflection and transmission coefficients characterize the discontinuities behaviour. Table 1 summarizes the values of such coefficients for a constant head reservoir, a terminal valve discharging in air, a Y junction and a leak. With particular reference to the applications shown in the following, it can be observed that a Y junction with pipes with the same A and a, has reflection and transmission coefficients respectively equal to $-1/3$ and $2/3$.

Because of partial reflection and transmission the number of waves propagating in the system can grow significantly with time. In order to simulate the pressure signal at

Table 1 | Values of the reflection (C_R) and transmission (C_T) coefficients for selected types of singularity (for the Y junction and the leak, the case of a pressure wave arriving from branch 1 is considered)

Singularity	C_R	C_T
Upstream reservoir	-1	0
Dead end	$+1$	0
Y junction	$\frac{\frac{A_1}{a_1} - \frac{A_2}{a_2} - \frac{A_3}{a_3}}{\frac{A_1}{a_1} + \frac{A_2}{a_2} + \frac{A_3}{a_3}}$	$\frac{\frac{2A_i}{a_i}}{\frac{A_1}{a_1} + \frac{A_2}{a_2} + \frac{A_3}{a_3}}$, $i = 2,3$
Leak	$-\frac{I_r}{2+I_r}$, $I_r = \frac{Q_L^-}{2Q_1^0}\frac{\Delta p^*}{p_L^-}$	$\frac{2}{2+I_r}$

any node, the paths and nodal arrival times of each wave must be memorized, leading to an exponential growth in the need for memory capacity as the simulation advances. It is also true that, by establishing a threshold value of wave amplitude (even one that is rather low) below which pressure waves do not propagate, these memory requirements can be significantly reduced. The final phase of reconstructing the pressure history at a point entails identifying which waves, from among the many archived in the memory, have passed the point, calculating the exact moment of passage and introducing the attendant variations with the appropriate amplitude.

WAVELET ANALYSIS

The complete wavelet transform of the continuous signal $s(t)$ can be defined as:

$$W_\lambda s = \int_{-\infty}^{+\infty} s(t)\psi_\lambda(t-\mu)\mathrm{d}t \tag{10}$$

that is, as the convolution of $s(t)$ with the 'dilation' of a function $\psi(x)$, the wavelet:

$$\psi_\lambda(t) = \frac{1}{\lambda}\psi\left(\frac{t}{\lambda}\right) \tag{11}$$

The two parameters λ and μ, respectively known as the *scale* and *translation* parameters, permit exploration of the signal at different temporal scales.

Since the signals to be analysed usually comprise a series of data obtained from discontinuous sampling and variable manipulation, in practice the wavelet transform is not calculated with Equation (10) but with its corresponding discrete form in the time domain, in a manner analogous to the preferential use of the discrete Fourier transform in Fourier analysis. Beyond considering a discontinuous signal, sampled at constant frequency for a limited number of time increments N,

$$s(i\Delta t), \quad i = 0, \ldots, N-1 \tag{12}$$

with $\Delta t =$ sampling period, it is possible to discretize the parameters λ and μ. All of the transforms subsequently presented are obtained by means of the wavelet transform of Mallat & Zhong (1992), indicated as *MZWT*, with

$$\psi(t) = \begin{cases} 0 & 1 \le |t| \\ \psi(-t) & 0 \le t < 1 \\ -24t^2 - 16t & -0.5 \le t < 0 \\ 8(t+1)^2 & -1 < t < -0.5 \end{cases} \tag{13}$$

which is an approximation of the first derivative of the Gaussian function.

This transform, which is semi-discrete on the dyadic scale ($\lambda = 2^j$), is furnished by the sum of terms:

$$W_{2^j}s(i\Delta t) = \frac{1}{2^j}\sum_{k=0}^{N-1} s(k\Delta t)\psi\left(\frac{(k-i)\Delta t}{2^j}\right) \quad j = 1, 2, \ldots, J \tag{14}$$

with $J < \log_2 N$ plus a final term of approximation $S_J(i\Delta t)$. The information contained in the JxN values for which the transform is defined is redundant. This contrasts with orthogonal wavelet transforms for which, as the scale expands, the number of instants in which the transform is calculated diminishes and so too does the number of coefficients. It is for this reason that if wavelet analysis generally allows for the exposure of singularities present in a signal by filtering noise, the *MZWT* is especially well suited to this purpose. The wavelet transform of a signal is equal to the first derivative of the convolution of the signal with a smoothing function $\phi(t)$ such that $\psi(t) = (\mathrm{d}\phi(t)/\mathrm{d}t)$. Thus, the most rapid signal variations adjusted by the smoothing function, and also their discontinuities, are equal to the maximum local moduli of the wavelet transform. Thanks to procedures described by Mallat & Hwang (1992) and Donoho (1995), it is possible to filter noise which degrades the information content of experimental signals and to improve the identification of singularities: in correspondence to these, the maximum local moduli of the wavelet transform appear in typical form with the variation of scales, organizing themselves into 'chains'. Such chains, by exposing singularities in the pressure signal, also identify the passage of waves through the measurement section, even if this is marked by a modest fluctuation in pressure. The choice of the *MZWT* enhances analysis by minimizing the adverse effects that could introduce disturbance to the signal.

THE LABORATORY SET-UP AND TESTS

Experimental tests were carried out at the Water Engineering Laboratory (WEL) of the Department of Civil and Environmental Engineering (DICA) at the University of Perugia, Italy. The HDPE laboratory pipe of nominal diameter DN110 is configured in a Y shape, with three links and four nodes: the Y junction (Y), the supply tank (R), the dead end (D) and the connection with the device generating the pressure wave (P) (Figure 1).

At the supply tank, pressure is maintained constant by varying pump speed in relation to the supplied flow. The tank is connected to the Y junction across branch 3 which has a length $L_3 = 197.82$ m. In turn, the junction is connected by means of branch 2 (of length $L_2 = 116.78$ m) to the dead end D and by means of branch 1 ($L_1 = 61.78$ m) to an apparatus able to generate pressure waves at P. Such an apparatus can be either a valve or the PPWM device (portable pressure wave maker), recently developed and refined at the DICA (Brunone *et al.* 2008). This consists of a steel tank filled with water and air in which pressure is brought, via a compressor, to a preset level above that in the pipe. The device is connected to the test pipe with a small valve whose rapid opening generates a pressure wave that propagates through the system. When PPWM is connected to an intact system, the initial conditions can include the absence of flow in all branches (i.e. hydrostatic conditions). In the following, the PPWM device is used for laboratory tests, whereas in the real system tests are performed with a valve.

Pressure measurements were undertaken at a sampling frequency of 200 Hz in two different sections: the first, located immediately upstream of section P, corresponding to the connection between the PPWM device and branch 1; the second immediately upstream of the dead end D and branch 2. The first test refers to an intact (i.e. leak-free) system. Figure 2 shows the pressure signals registered at sections P (Figure 2(a–d)) and D (Figure 2(e–h)). The time $t = 0$ s refers to the start of opening of the PPWM valve. Figure 2(b) reports the time behaviour of the *MZWT* of the pressure signal in Figure 2(a) for $j = \log_2\lambda$. For greater clarity, and to facilitate subsequent comparisons, Figure 2(c) shows the wavelet transform of Figure 2(b) for an assigned scale value ($j = 6$). Scrutiny of these figures reveals other singularities occurring after the instant of the transient generating manoeuvre $t = t^W_{1,P} = 0$ s. These occur at

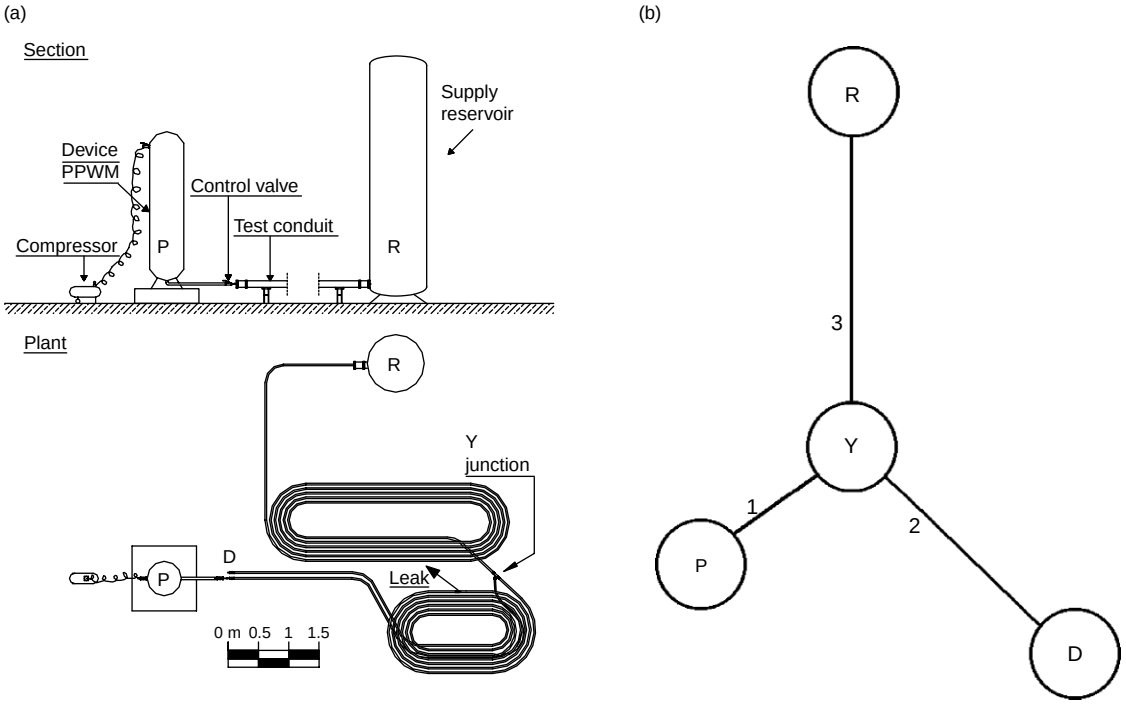

Figure 1 | (a) Experimental set-up at the Water Engineering Laboratory of the DICA—University of Perugia; (b) outline of the system as a Y structure.

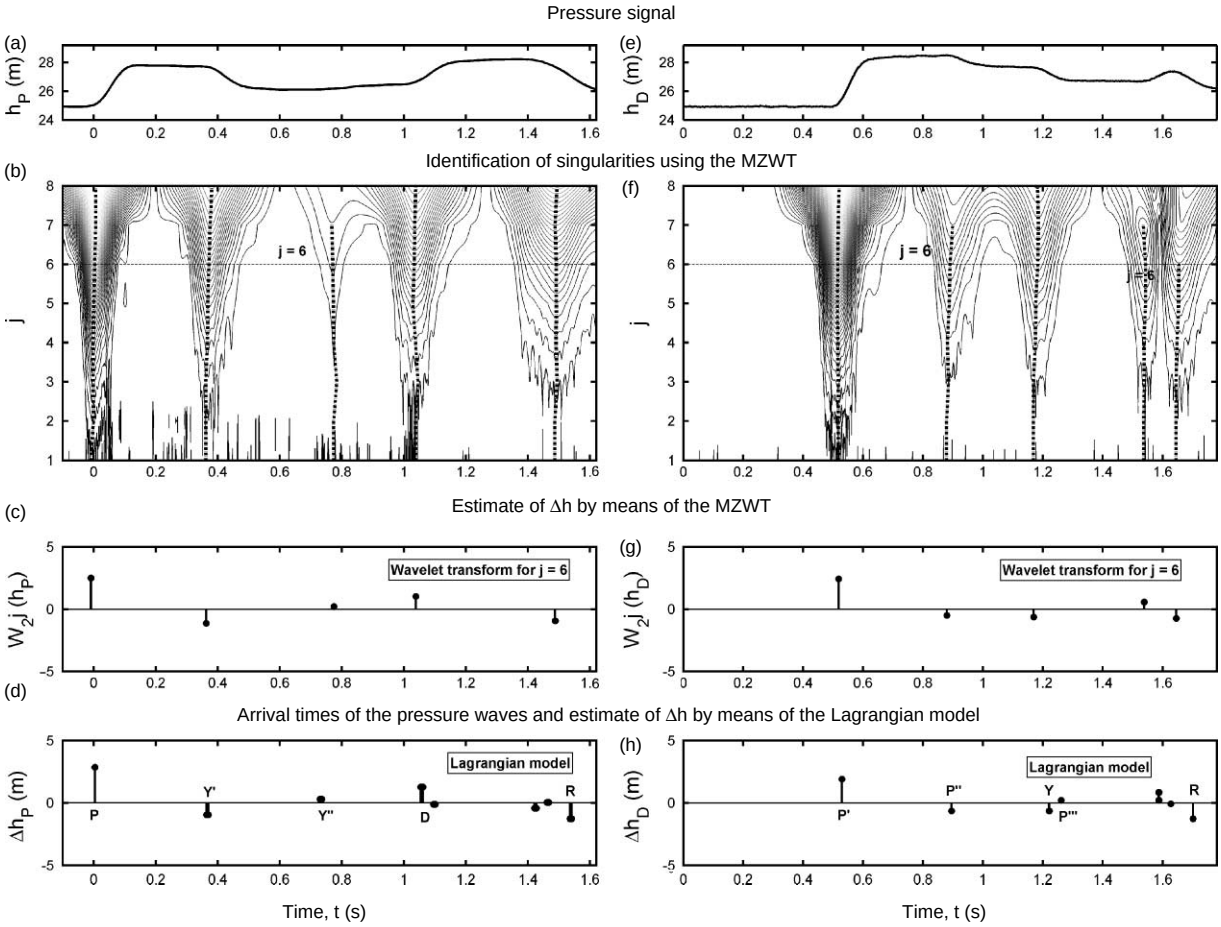

Figure 2 | System assessment for intact pipes: (a–d) measurement section P; (e–h) measurement section D.

$t = t^W_{2,P} = 0.366\,\text{s}$, $t = t^W_{3,P} = 0.779\,\text{s}$, $t = t^W_{4,P} = 1.043\,\text{s}$ and $t = t^W_{5,P} = 1.492\,\text{s}$. The first subscript denotes the numerical sequence of the singularity, the second indicates the measurement section and the superscript confirms that these times were obtained via wavelet analysis. Interpretation of such discontinuities is facilitated by comparison with the results of the Lagrangian model. By dealing with pipes of the same characteristics, the only parameter of the calibration problem, the wave speed, can be calculated using the relationship $a = 2L_1/(t^W_{2,P} - t^W_{1,P})$. Figure 2(d) depicts the pressure variations observed in time at the measurement section as calculated by the Lagrangian model, indicating the arrival times and amplitudes of pressure waves traversing the section. It is evident that this graph substantially coincides with the impulse response function that can be obtained, for example, by integrating the equations of unsteady motion in the frequency domain (Wylie & Streeter 1993).

DISCUSSION OF THE LABORATORY RESULTS

Interpretation of Figure 2(d) can be simplified by comparison with Figure 3 which conceptualizes the propagation of pressure waves up to time $t_4 = 0.549\,\text{s}$, as derived by the Lagrangian model. Specifically, in the graphs of Figure 3, the position of the pressure waves travelling through the pipe system is reported at some significant times. Each graph is integrated with a table containing the name assigned to each wave (α, α_1, α_2…), the node of origin of the wave and its arrival or departure time at the node. Moreover, beneath each graph the pressure signal is given,

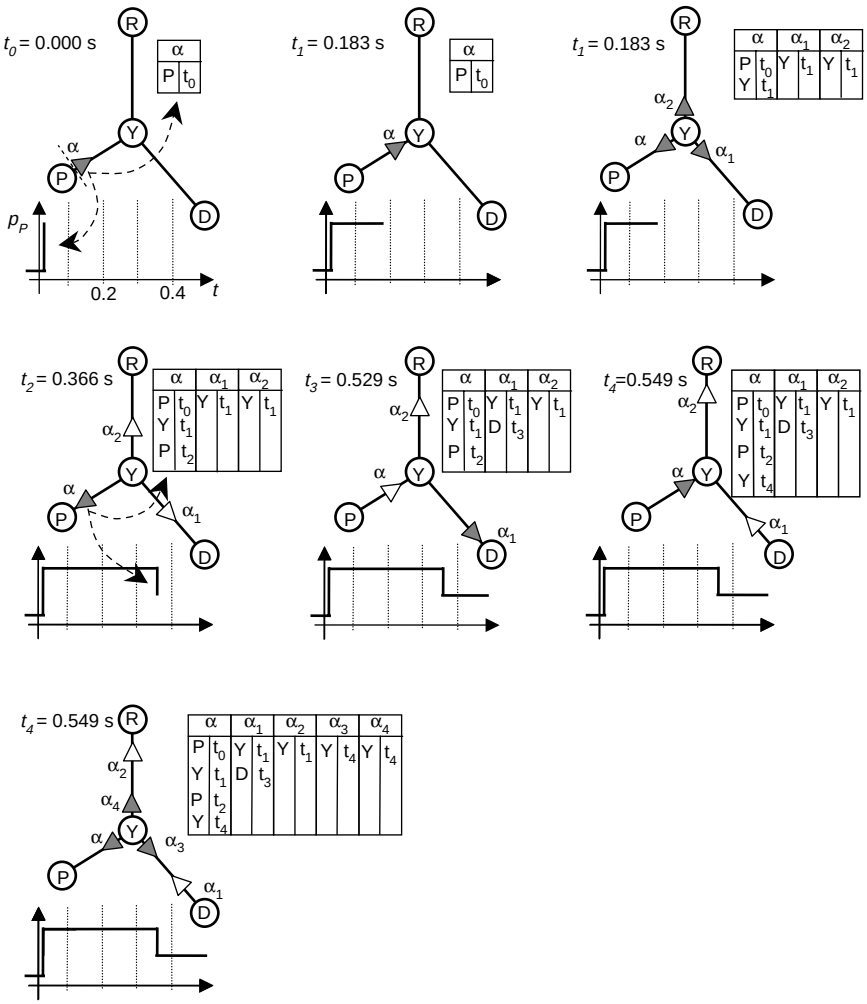

Figure 3 | The position of waves travelling through the system in graphic and tabular form along with the pressure signal at section P.

up to that instant, calculated at section P, where experimental data of Figure 2(a) were acquired.

The first graph of Figure 3 refers to $t = 0.000$ s and then only the pressure wave α generated by the PPWM is depicted. Such a pressure wave arrives at the Y junction at time $t = 0.183$ s. Therein, the incident wave splits in three: the first, α is reflected toward the section P, the second, α_1, and the third, α_2, are transmitted toward the dead end D and the reservoir R, respectively. For simplicity, the reflected waves are indicated with the same symbol as the relevant incident wave.

The wave α, reflected at the junction, arrives at section P at $t_{2,P} = 0.366$ s and determines a discontinuity on the pressure signal, the same discontinuity indicated by symbol Y′ in Figure 2(d). It should be noted that the symbol marking the discontinuity is the same of the singularity that reflected the wave. The wave α is newly reflected at section P and travels along branch 1 reaching the Y junction at $t = 0.549$ s, where once again three waves are generated: α, which is reflected towards P, and α_3 and α_4 which are sent towards D and R, respectively. Shortly before this happens, at $t_{1,D} = 0.529$ s, the wave α_1 arrives at the dead end D and is, in turn, reflected from it. Proceeding further with the description of wave multiplication, take for example the wave α_1 which is reflected by the dead end and arrives at Y at $t = 0.875$ s where it generates another three waves: α_1 is reflected towards D, and α_5 and α_6 are transmitted towards P and R, respectively. Owing to the greater length of branch 2 (YD) relative to that of branch 1 (PY), α reaches section P for the second time at $t_{3,P} = 0.732$ s. This takes place before

the arrival of α_5 which reaches the section P only at $t_{4,P} = 1.058$ s: α is thus also responsible for the presence of the third discontinuity labelled as Y″, while α_5 determines the singularity D. The wave α_2, coming from the tank, makes its appearance in section P at $t_{5,P} = 1.538$ s after having undergone reduction due to partial transmission at Y. It is evident that, because of the system's configuration and the location of the measurement section (the section P), all the waves are modified by the Y junction on the basis of the mechanisms just described.

The relative percentage error among the times $t_{i,P}$ (for $i = 1, \ldots, 6$) calculated by the Lagrangian model, and those determined by wavelet analysis, is always less than 2.5%. Thus, in this case, the Lagrangian model is able to accurately interpret the pressure time-history for the phases described and it seems possible to conduct effective diagnosis of a Y-configured system on the basis of an unsteady test characterized by a modest overpressure of only 2.95 m.

Similar diagnosis considerations also apply to the pressure signal observed at section D during the same test (Figure 2(e–h)). In particular, the Lagrangian model attributes to wave α_1 (which arrives in section D at $t_{1,D} = 0.529$ s) the discontinuity in the pressure signal indicated by symbol P′. This wave is once again reflected at D and at Y, appearing in section D at $t_{3,D} = 1.221$ s and giving rise to the discontinuity referred to as Y. Its advent in the section is preceded by the wave α_3 which arrives at $t_{2,D} = 0.895$ s and is associated with the discontinuity marked as P″. The wave α, which arrives at Y after two consecutive reflections, is once again reflected and spawns two new waves that are transmitted toward sections D and R, indicated as α_7 and α_8, respectively. The wave α_7 is responsible for the discontinuity at $t_{4,D} = 1.261$ s, labelled as P‴. Finally, at $t_{5,D} = 1.701$ s another discontinuity inflects the pressure wave. This is indicated by R and is due to the first wave α_2 which is reflected by the tank and transmitted to Y towards section D.

If the system is damaged (i.e. with a leak), the topological schema of the network used by the Lagrangian model differs from the preceding description by the addition of a leak-node somewhere on a link and by the division of this link into two parts. It is noted that the position of a leak on a link is arbitrary and there are no constraints with respect to a specific position, as is the case with a model based on the MOC. In the shown tests referring to a damaged system, the same experimental set-up is kept, but with a leak of diameter $d = 1.49$ cm on branch 1 at 24.68 m distance from section P. The wavelet analysis of the experimental signal (Figure 4(a)) recorded at section P identifies a chain (denoted by the letter L) in Figure 4(b) that is absent in the corresponding signal for the intact system shown in Figure 2(a). Exploiting information regarding topology and pipe characteristics obtained from the intact system, by means of the Lagrangian model it is possible to discern the position and the characteristics of the leak and simulate the pressure signal (Figure 4(c)). In Figure 4(c), a numerical simulation of the same pressure signal obtained by a frictionless MOC is shown (dashed line), confirming that the results obtained by the two models practically coincide.

Analogously, when the same leak is placed on branch 2, at a distance 92.43 m from section D, wavelet analysis of the signal measured at section D (Figure 5(a)) unearths a new chain, indicated by L in Figure 5(b), that was not present in Figure 2(f) at $t = 1.088$ s. The numerical simulation (Figure 5(c)) associates this chain to the arrival in the measurement section of the wave generated by the manoeuvre, which was transmitted to the junction Y and to the leak, and thus reflected at the dead end and at the leak.

Such a leak can be clearly identified even should the measurement be undertaken at section P. Notwithstanding its clarity from the numerical reconstruction, the wave reflected at the leak is attenuated by the presence of the junction at Y, reaching measurement section P at $t = 0.49$ s with an amplitude, as calculated by the Lagrangian model, of only 0.57 m. It is evident that in a Y system, at least two measurements in different links are required in order to proceed with localizing the singularity. Conversely, by taking only one measurement from only one branch, it would not be possible to distinguish in which of the other two links a potential singularity revealed by the pressure signal may be located, or from which of the two branches, beyond the junction, comes the reflected wave. It should be pointed out that this circumstance does not arise from a model limitation but from physical constraints. It would be similarly difficult, despite an extensive search, to determine the position of an acoustic source listening only to a

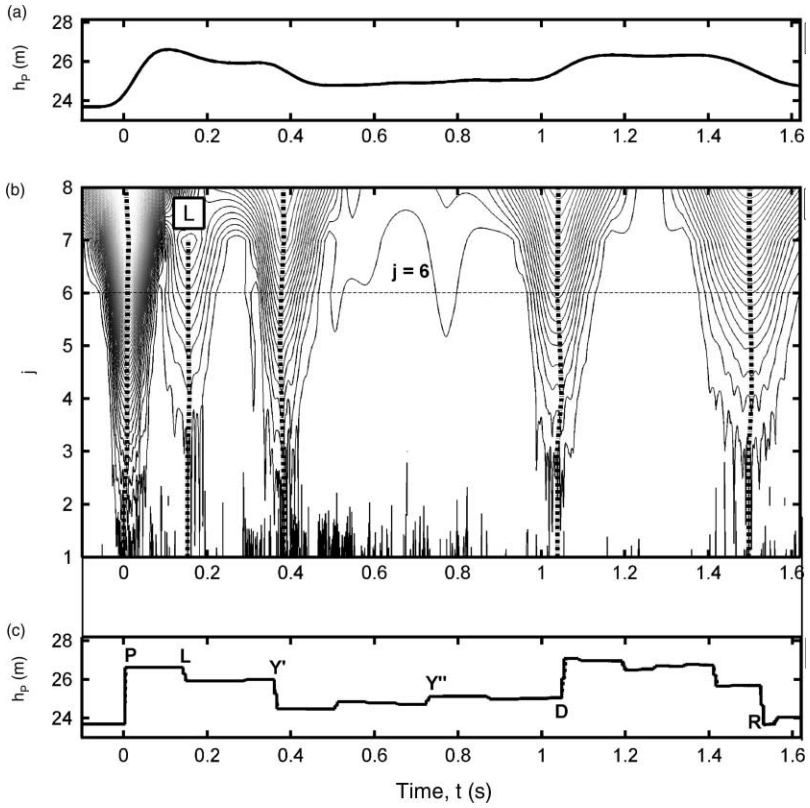

Figure 4 | Analysis of the system with damaged pipes (leak on link 1), (a) pressure signal recorded at measurement section P; (b) diadic wavelet transform of the pressure signal; (c) numerical reconstruction carried out by the Lagrangian model (continuous line) and by MOC (dashed line).

recording produced by a single fixed microphone in the absence of stereo.

FIELD TESTS

Since reliability of transient-test based techniques for leak detection have been assessed via numerical and laboratory experiments, the execution of field tests plays a crucial role for the implementation of the proposed method in practice. As a matter of fact, field tests can reveal possible criticalities of the approach as well as suggest a proper test procedure.

The examined real system is the Lintrathen East Trunk Main near Balmashanner, Scotland, managed by Scottish Water (Figure 6(a) and (b)). The system is in a Y configuration: branch 1, which spans nodes V and Y, joins the Balmashanner reservoir (node V) to the trunk main joining Lintrathen to Framedrum (the dashed line in Figure 6(a)) and has a diameter of 300 mm and length $L = 5{,}936$ m, while branches 2 and 3 are part of the same trunk main with 700 mm diameter and have lengths of 5,223 and 694 m, respectively. All the system pipes are in ductile iron. The considered test was carried out within the European Project *Surge-Net* as a 'blind' test, to check innovative methods for leak detection. During the test, the Balmashanner reservoir was temporarily disconnected from the system by closing valve V_1 (Figure 6(b)) and the total closure manoeuvre was executed at the hydrant valve V situated in the immediate vicinity. A drain was purposely left open to simulate the presence of a leak at a distance of 3,100 m.

Figure 6(c) reproduces the pressure signal registered by a pressure transducer (at 20 Hz) upstream of the valve V. The wavelet analysis of the signal (Figure 6(d)) distinguishes three chains at times $t_1^W = 5.45$ s, $t_2^W = 10.65$ s, and $t_3^W = 15.25$ s, indicated by the letters V, L′ and Y′. The Lagrangian model (Figure 6(e)) respectively attributes the first and the last chains, V and Y′, to the passage of the positive pressure wave generated by the valve

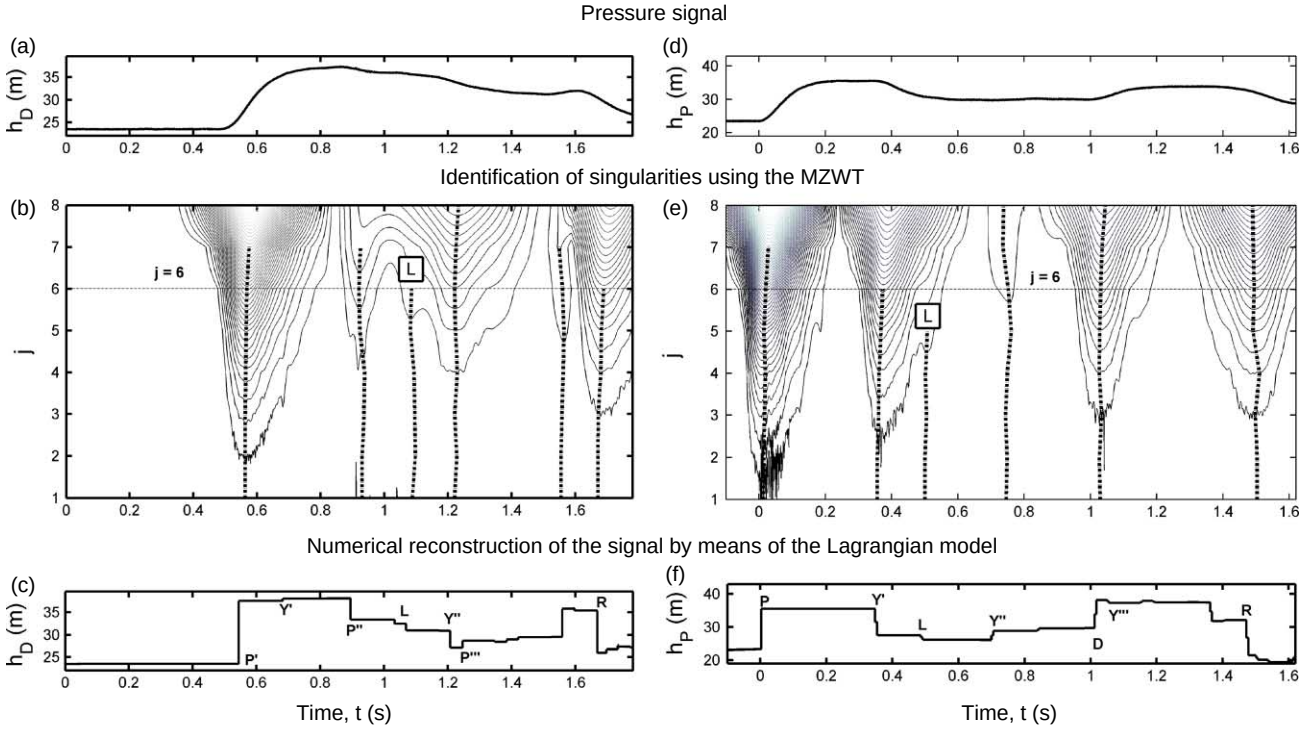

Figure 5 | Analysis of a damaged system with a leak on link 2: (a–c) measurement section D; (d–f) measurement section P.

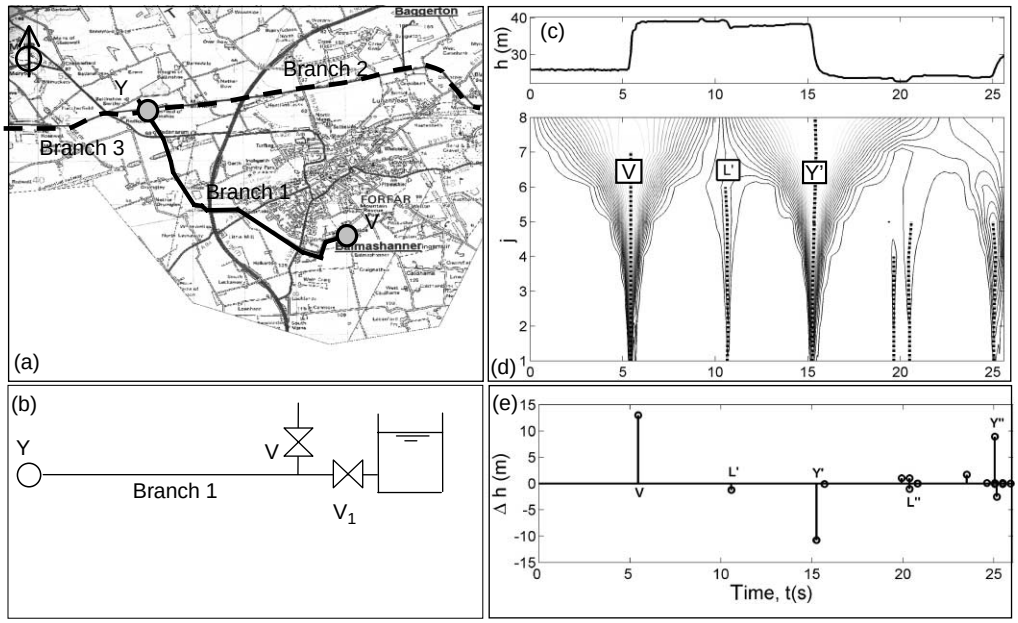

Figure 6 | (a) Topographic representation of the trunk main system studied in the field investigation, with the segment of branch 1 (unbroken line from V to Y) and branches 2 and 3 which are part of the Lintrathen–Framedrum trunk main (dashed line); (b) schematic of branch 1; (c) pressure signal recorded upstream of valve V in (b) and (d) its wavelet transform (the black dashed lines correspond to the chains); (e) arrival times of the pressure waves and estimate of the amplitude of pressure change by means of the Lagrangian model.

closure and the wave reflected at the junction. Given the length of branch 1, the difference $t_3^W - t_1^W$ permits estimation of the pipe's wave speed $a = 1{,}211.43\,\mathrm{m\,s^{-1}}$.

The second chain can be attributed to the passage of a wave reflected from the simulated leak on branch 1. Knowing the value of a and the time interval between arrival of the wave generated at the valve and that reflected by the leak, the position of the singularity is estimated as 3,149 m from the measurement section, with a relative error less than 2% despite the low sampling frequency with which the signal was recorded.

CONCLUSIONS

Reliability of a transient test-based approach for the diagnosis of branched pipe systems has been inspected in both laboratory and real systems configured in a Y shape. Laboratory tests were carried out at the Water Engineering Laboratory of the University of Perugia (I) on a HDPE pipe; field tests were executed at the Lintrathen East Trunk Main (Balmashanner, Scotland). Pressure waves were generated by closing a valve or by means of the PPWM device developed by the authors; in both cases small amplitude overpressures (i.e. only a few metres of head) characterized transients.

Analysis of the pressure signals was carried out by coupling wavelet functions and a Lagrangian model. The Lagrangian model memorizes the amplitude of each wave and the moment in which it passes the singularities, transferring the information about singularities position and characteristics in the simulated pressure signal. Wavelet analysis allows for pointing out singularities in pressure signals due to the presence of singularities (e.g. leaks). Hence, the Lagrangian model transforms the rapid variations detected by the wavelet analysis in the pressure signal, in system singularities location and characteristics.

Experimental pressure signal interpretation confirms the validity of the approach and encourages further development and refinement. Moreover it has revealed some aspects of the proposed approach. Firstly, despite the assumption of frictionless fluid in the Lagrangian model, the method can be effective by extending the simulation to the moment in which the wave that has reached the furthest extremity of the system (in terms of travel time) arrives at the measurement section. In so doing, the entire system is explored and the location of singularities can be obtained. Secondly, in a branched system the number of measurement sections must increase with the number of junctions since for each junction it is not possible to distinguish in which of the two links a potential singularity revealed by the pressure signal may be located. The necessary increase in the number of measurement sections can moderate the effect of the junctions, which cause the damping of the pressure waves and can significantly diminish their amplitude–especially when such attenuation is exacerbated by the successive passage of the same wave across other junctions.

ACKNOWLEDGEMENTS

The research is in part based on results obtained from the Thematic Network 'Surge-Net' (ref. G1RT-CT-2002-05069) financed under the Fifth Framework Programme 'Growth' of the European Community. The authors are the sole persons responsible for the contents of this article and acknowledge that such contents do not necessarily reflect the opinion of the Community. The Community is not responsible in any way for the use of the data provided herein or for any consequences arising from its use. The authors thank the following project partners for assistance in collecting field data: A. Young, and D. Covas and H. Ramos of the Istituto Superior Técnico of Lisbon.

This research has been jointly supported by the Italian Ministry of Education, University and Research (MIUR) under the Project of Relevant National Interest "Innovative criteria for the sustainable management of water resources in the water distribution systems", and by Fondazione Cassa Risparmio Perugia.

REFERENCES

Brunone, B. 1989 Una tecnica per la verifica dell'integrità di emissari sottomarini. *Immissione di acque reflue in mare*, CUEN, Napoli, D 223–236.

Brunone, B. 1999 Transient test-based technique for leak detection in outfall pipes. *J. Water Res. Pl-ASCE* **125**(5), 302–306.

Brunone, B. & Ferrante, M. 2001 Detecting leaks in pressurised pipes by means of transients. *J. Hydraul. Res.–IAHR* **39**(5), 539–547.

Brunone, B. & Ferrante, M. 2004 Pressure waves as a tool for leak detection in closed conduits. *Urban Water J.* **1**(2), 145–155.

Brunone, B., Ferrante, M. & Meniconi, S. 2008 A portable pressure wave-maker for leak detection and pipe survey. *J. Am. Water Works Assoc.* **100**(4), 108–116.

Covas, D., Ramos, H. & Betamio de Almeida, A. 2000 Leak location in pipe systems using pressure surges. In: *8th International Conference on Pressure Surges*. Mechanical Engineering Publications, Bury St Edmunds (UK), pp. 169–179.

Donoho, D. L. 1995 De-noising by soft-thresholding. *IEEE Trans. Inform. Theory* **41**(3), 613–627.

Ferrante, M. & Brunone, B. 2003*a* Pipe system diagnosis and leak detection by unsteady-state tests. 1. Harmonic analysis. *Adv. Water Resour.* **26**(1), 95–105.

Ferrante, M. & Brunone, B. 2003*b* Pipe system diagnosis and leak detection by unsteady-state tests. 2. Wavelet analysis. *Adv. Water Resour.* **26**(1), 107–116.

Ferrante, M., Brunone, B. & Meniconi, S. 2007 Wavelets for the analysis of transient pressure signals for leak detection. *J. Hydraul. Eng.–ASCE* **133**(11), 1274–1282.

Greyvenstein, B. & van Zyl, J. E. 2007 An experimental investigation into the pressure-leakage relationship of some failed water pipes. *J. Water Suppl. Res. Technol.–AQUA* **56**(2), 117–124.

Gudmundsson, J. S., Durugut, I., Rønnevig, J., Korsan, K. & Celius, H. K. 2002 Pressure pulse analysis of flow in tubing and casing of gas lift wells. *Spring ASME/API Gas Lift Workshop*, Houston, Texas.

Jonsson, L. & Larson, M. 1992 Leak detection through hydraulic transient analysis. *International Conference on Pipeline Systems*. Kluwer Academic Publisher, Dordrecht, The Netherlands, pp. 273–286.

Kapelan, Z., Savic, D. A. & Walters, G. A. 2003 A hybrid inverse transient model for leakage detection and roughness calibration in pipe networks. *J. Hydraul. Res.–IAHR* **41**(3), 481–492.

Liggett, J. A. & Chen, L.-C. 1994 Inverse transient analysis in pipe networks. *J. Hydraul. Eng.–ASCE* **120**(8), 934–955.

Mallat, S. G. & Hwang, W. L. 1992 Singularity detection and processing with wavelets. *IEEE Trans. Inform. Theory*. **38**, 617–643.

Mallat, S. G. & Zhong, S. 1992 Characterization of signals from multiscale edges. *IEEE Trans. Pattern Anal.* **14**(7), 710–732.

Nicholas, R. E. 1990 Leak detection on pipelines in unsteady flow. *Forum on Unsteady Flow*. ASME, New York, pp. 23–25.

Stephens, M., Vítkovský, J. P., Lambert, M., Simpson, A. R., Karney, B. W. & Nixon, J. 2004 Transient analysis to assess valve status and topology in pipe networks. *In 9th International Conference on Pressure Surges*. BHR Group Limited, Cranfield, UK, pp. 211–224.

Stoianov, I., Karney, B. W., Covas, D., Maksimovic, C. & Graham, N. 2001 Wavelet processing of transient signals for pipeline leak location and quantification. In: *6th International Conference on Computing and Control for the Water Industry–CCWI 2001*, Leicester, UK, pp. 65–76.

van Zyl, J. E. & Clayton, C. R. I. 2007 The effect of pressure on leakage in water distribution systems. *Water Manage.* **160**(2), 109–114.

Wylie, E. B. & Streeter, V. L. 1993 *Fluid Transients in Systems*. Prentice-Hall, Englewood Cliffs, New Jersey.

First received 21 February 2007; accepted in revised form 15 August 2008. Available online January 2009